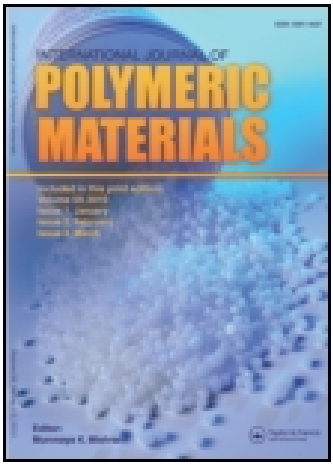

International Journal of Polymeric Materials and Polymeric Biomaterials

Publication details, including instructions for authors and subscription information:
http://www.tandfonline.com/loi/gpom20

Theory of Transient Permeation Through Reactive Barrier Films III. Solute Ingress Dynamics and Model Lag Times

Stanislav E. Solovyov [a] & Anatoliy Ya. Goldman [a]

[a] Department of Materials and Processing , Alcoa Closure Systems International, Inc. , Crawfordsville, Indiana, USA

Published online: 01 Sep 2006.

To cite this article: Stanislav E. Solovyov & Anatoliy Ya. Goldman (2005) Theory of Transient Permeation Through Reactive Barrier Films III. Solute Ingress Dynamics and Model Lag Times, International Journal of Polymeric Materials and Polymeric Biomaterials, 54:2, 117-139, DOI: 10.1080/00914030390245767

To link to this article: http://dx.doi.org/10.1080/00914030390245767

International Journal of Polymeric Materials, 54:117–139, 2005

ISSN: 0091-4037 print/1543-5253 online
DOI: 10.1080/00914030390245767

Taylor & Francis
Taylor & Francis Group

THEORY OF TRANSIENT PERMEATION THROUGH REACTIVE BARRIER FILMS III. SOLUTE INGRESS DYNAMICS AND MODEL LAG TIMES

Stanislav E. Solovyov
Anatoliy Ya. Goldman
Department of Materials and Processing,
Alcoa Closure Systems International, Inc.,
Crawfordsville, Indiana, USA

Parts I and II of this series formulated theoretical foundations of transient permeation through reactive barrier films with finite reactive capacity to bind permeating solute [1,2]. In Part III the methodology of transient ingress analysis is introduced based on the SG model of transient permeation. The lag time concept for non-catalytic reactive films is clarified. The concept of the SG model lag time is introduced as a convenient engineering parameter for evaluating the barrier performance of reactive films within fintie timeframes. The experimental methods of determining scavenging reaction rates are discussed when the scavenger is available in a free form. The synergistic effects of permeant diffusivity, solubility in film material and scavenger reactivity on the effective transmission rate of the solute permeation are quantified by comparing representative single layer films with the same scavenger loadings. It is demonstrated that placing the scavenger within a material with the lowest diffusivity, provided the passive transport properties of compared films are the same, is the optimal choice resulting in the lowest transient transmission rate until the scavenger reactive capacity is exhausted. The terminology, notation and section numbering continue from Parts I and II of the paper.

Keywords: reactive barrier, oxygen scavenger, transient permeation, ingress, multilayer, scavenger exhaustion time, lag time, lead time, optimized layer sequence

Received 2 July 2003; in final form
The authors thank Prof. Witold Brostow of the University of North Texas for useful comments and suggestions during manuscript preparation.

Address correspondence to Dr. Stanislav E. Solovyov, Multisorb Technologies, Inc., 325 Harlem Road, Buffalo, NY 14224, USA. E-mail: ssolovyov@multisorb.com

17. SOLUTE INGRESS MODEL

Part II described a model of transient permeation through noncatalytic reactive membrane (SG model). The accuracy of SG model predictions can be checked by comparing the model predicted solute ingress I into the package during time $t^* < t_E^+$ (t_E^+ is the SG model scavenger exhaustion time) found as

$$I(t^*) = -\int_0^{t^*} J_0(t)dt \tag{17.1}$$

with numerical simulations. The ingress I describes the amount of solute exited from the unit area of the reactive membrane into the package during specified time: that is why the effective flux J_0 across downstream film boundary is used in Eq. 17.1. The negative sign in Eq. 17.1 appears because of defining the negative flux according to Fick's first law of diffusion in the presence of positive solute pressure gradient across the film, but the ingress should obviously have a positive value. The effective flux J_0 is found from SG model result (Eq. 10.11) presented in Part II as

$$\begin{aligned} -J_0(t) &= \frac{2C_{out}\sqrt{kD}\,\exp\left(L_d\sqrt{k/D}\right)}{\left(1+\exp\left(2L_d\sqrt{k/D}\right)\right)\left(1+(L-L_d)\sqrt{k/D}\right)^{-2}} \\ &= \frac{DC_{out}}{L}\frac{2\phi_0 e^{\phi}}{(1+e^{2\phi})(1+\phi_0-\phi)^{-2}} \end{aligned} \tag{17.2}$$

where ϕ is the transient Thiele modulus:

$$\phi = L_d(t)\sqrt{\frac{k}{D}} \tag{17.3}$$

$L_d(t)$ is the reaction wavefront position, and ϕ_0 is the initial Thiele modulus $\phi_0 = L\sqrt{k/D}$. The implicit SG model solution for $L_d(t)$ is represented by Eq. 15.11 in Part II and reproduced here. When the reaction wavefront approximation is valid and $C_{in} = 0$, the time to reach the wavefront position L_d ($L_d = L$ and $t = 0$) is

$$t = \frac{\mu R_0}{C_{out}}\left[\frac{(L-L_d)^2}{2D} - \frac{L-L_d}{\sqrt{kD}} + \frac{1}{k}\ln\left(\frac{1+\exp\left(2L\sqrt{k/D}\right)}{1+\exp\left(2L_d\sqrt{k/D}\right)}\right)\right] \tag{17.4}$$

where $\mu = C/R$ is the scavenger reactive capacity defined as the stoichiometric coefficient for the amount of the permeating species

consumed by a given amount of the scavenger. When the scavenger capacity is exhausted, the steady state flux across any plane $x = \text{const}$ within a homogeneous monolayer film is

$$-J_x = TR_{eff}\Delta p = \frac{DS\Delta p}{L} \tag{17.5}$$

where $\Delta p = p_{out} - p_{in}$, and the ingress through the passive barrier is found from Eq. 17.1 as

$$I_p(t) = \frac{DS\Delta p}{L}t = \frac{D}{L}C_{out}t \tag{17.6}$$

for $C_{in} = 0$. Substituting Eqs.17.2 and 17.4 into Eq. 17.1 and replacing integration by t with integration by dimensionless wavefront position coordinate $\xi = L_d/L = [1..0]$ with corresponding integration limits change, after routine rearrangements the ingress during the scavenger exhaustion time ($t^* \le t_E^+$) is

$$\begin{aligned} I_R(\xi^*) &= 2\mu R_0 L \int_{\xi^*}^{1} \frac{e^{\phi_0\xi}[(1+e^{2\phi_0\xi})\phi_0(1-\xi) + e^{2\phi_0\xi} - 1]}{(1+e^{2\phi_0\xi})^2(1+\phi_0(1-\xi))}d\xi \\ &= 2\mu R_0 L \left(\frac{\arctan(e^{\phi_0\xi})}{\phi_0}\bigg|_{\xi^*}^{1} - \int_{\xi^*}^{1} \frac{2e^{\phi_0\xi}}{(1+e^{2\phi_0\xi})^2[1+\phi_0(1-\xi)]}d\xi \right) \end{aligned} \tag{17.7}$$

The remaining integral in Eq. 17.7 cannot be taken analytically; however, its lower bound can be estimated so that the upper bound estimate of total ingress $I_R(t)$ can be obtained for practical purposes. We note that for $\xi = [1..0]$, the square bracketed expression in the integral (Eq. 17.7) denominator is bound by:

$$1 \le [1 + \phi_0(1-\xi)] \le 1 + \phi_0 \tag{17.8}$$

If it is replaced by the upper bound $1 + \phi_0$, then the integral in Eq.17.7 becomes analytical and the upper estimate of the ingress as a function of time is

$$\begin{aligned} I_R^+(\xi^*) &= \frac{2\mu R_0 L}{1+\phi_0}\left(\arctan(e^{\phi_0\xi}) - \frac{e^{\phi_0\xi}}{\phi_0(1+e^{2\phi_0\xi})}\right)\bigg|_{\xi^*}^{1} \\ &= \frac{2\mu R_0 L}{1+\phi_0}\left(\arctan(e^{\phi_0}) - \arctan(e^{\phi_0\xi^*}) - \frac{e^{\phi_0}}{\phi_0(1+e^{2\phi_0})} + \frac{e^{\phi_0\xi^*}}{\phi_0(1+e^{2\phi_0\xi^*})}\right) \end{aligned} \tag{17.9}$$

For the upper estimate of the ingress during the scavenger exhaustion time (at $t = t_E^+$, i.e., $\xi^* = 0$) we obtain

$$I_R^+(t_E^+) \equiv I_R^+(\xi^* = 0) = \frac{2\mu R_0 L}{1+\phi_0}\left(\arctan(e^{\phi_0}) - \frac{\pi}{4} - \frac{e^{\phi_0}}{\phi_0(1+e^{2\phi_0})} + \frac{1}{2\phi_0}\right) \tag{17.10}$$

For a large initial Thiele modulus ϕ_0, the upper estimate of the ingress during t_E^+ asymptotically approaches its lower limit:

$$L_R^+(\phi_0 \to \infty) = \frac{\mu R_0 \pi L}{2(1+\phi_0)} \tag{17.11}$$

Note that the ingress in Eqs.17.10 and 17.11 does not depend on the boundary conditions (it is true only when the case of fixed $p_{in} = 0$ is considered). The exhaustion lag time t_{LE} for the reaction rate $k \to \infty$ first derived by Cussler and Yang [3–4] and easily obtained from general result (Eq. 17.4) is

$$t_{LE} = \frac{\mu R_0}{C_{out}}\frac{L^2}{2D} = \frac{\Psi\phi_0^2}{2k} \tag{17.12}$$

where dimensionless parameter Ψ is the relative scavenging capacity of the film material defined as

$$\Psi = \frac{\mu R_0}{C_{out}} \tag{17.13}$$

The solute concentration C_{out} within the outside membrane boundary can be related to the solute partial pressure outside the package using the sorption isotherm suitable for the specific experimental conditions. For linear sorption isotherm the relationship is simply $C_{out} = Sp_{out}$. As seen in Figure 1, an excellent agreement of Eq. 17.10 with numerical simulations is obtained for $\phi_0 > 2$. In Figure 1 t_E^+ is found as a function of ϕ_0 according to the SG model result (Eq. 16.1) in Part II. Line "P" corresponds to the ingress through P-film at steady state permeation conditions during t_E^+ with steady initial conditions (Eq. 2.9). Line "R-Num" is the ingress through noncatalytic R-film obtained by numerical simulations. Line "R-SG" follows the ingress prediction according to the SG model with the dashed part corresponding to model break down at $\phi_0 < 2$. The apparent deviation of numerical ingress from SG model results at $\phi_0 > 30$ is due to the fact that SG model predicts the ingress assuming the solute concentration profile instantly adjusting from passive to reactive permeation at the moment of scavenger

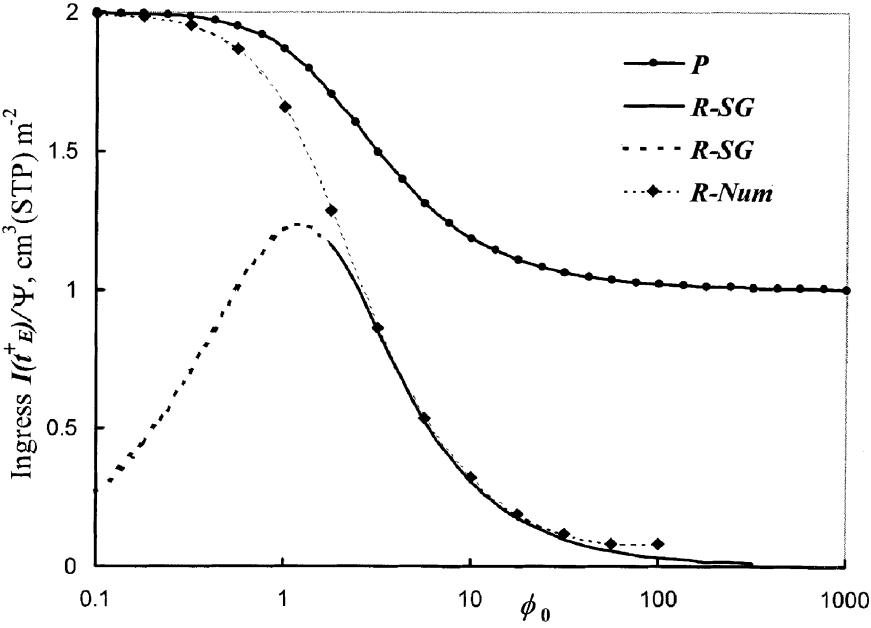

FIGURE 1 Ingress through R-film during SG model scavenger exhaustion time t_E^+.

activation at $t = 0$, that is the difference between the solute amount initially present in the passive film and the solute amount present in the reactive film in (pseudo) steady state upon instantaneous scavenger activation is assumed to be instantly consumed, disappearing without affecting the scavenger capacity (as shown in Figure 2). In actual systems this transition from passive steady state to reactive pseudo steady state (thereafter, P-R transition) is not instantaneous even if the scavenger is activated instantly. Moreover, a significant solute amount will exit into the package across $x = 0$ boundary during the P-R transition time generating the additional ingress exhibited in numerical simulations. The effect of scavenger activation kinetics on transient ingress is not considered in this work. This kinetics can be nearly instantaneous as in activation by UV light or rather slow as in activation by moisture diffusion through the film, resulting in additional complexity of initial transitions. Also, even though the effects of scavenger activation and P-R transition on the transient ingress may be significant, the contribution of these effects to the preceding ingress during passive permeation period usually can be neglected. Therefore this article will not be concerned with deviations

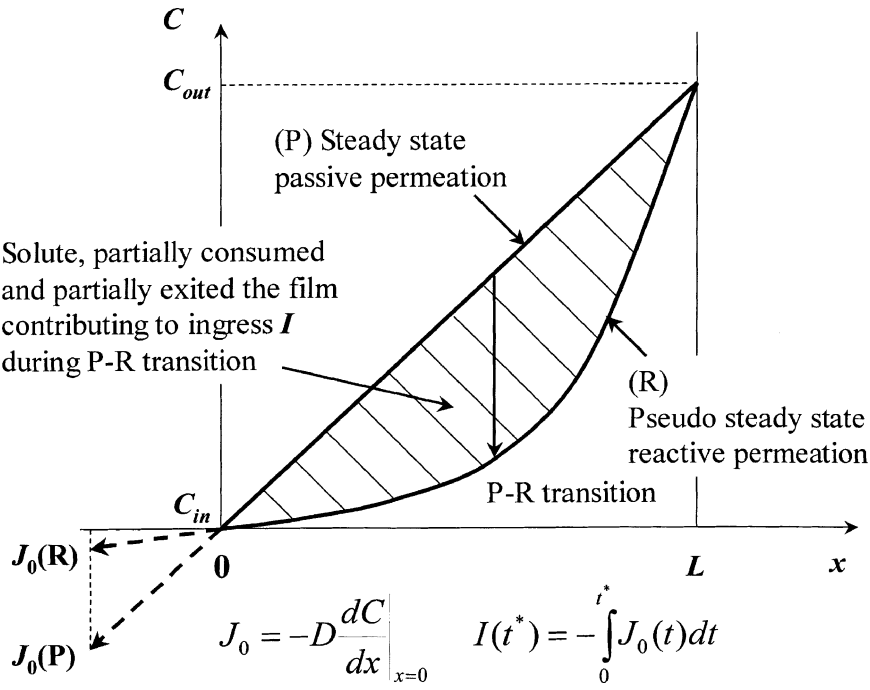

FIGURE 2 Effect of transition from passive to reactive permeation on solute ingress.

from the theory stemming from P-R transition and scavenger activation kinetics.

The ingress after t_E^+ can be approximated by the passive barrier solution after scavenger capacity exhaustion as in Eq. 17.6. Total ingress during $t > t_E^+$ that includes reactive and passive permeation periods is simply a sum of results in Eqs. 17.10 and 17.6:

$$I(t) = I_R(t_E^+) + I_P(t - t_E^+) \tag{17.14}$$

Whereas for $t < t_E^+$ Eq. 17.4 should be numerically solved for $L_d(t)$ and then Eq. 17.9 is used to find the ingress after substitution $\xi^* = L_d/L$.

18. STEADY STATE LEAD AND LAG TIMES

After the method for evaluating permeant ingress was established in Section 17, it might be interesting to determine the reference lag time for noncatalytic non-instantaneous reaction following the lag time

definition for passive barriers. However, before using the approximate SG solution for the ingress, this article applies fundamental principles to determine the lag time trends as a function of nonzero reaction rate $k > 0$ and finite scavenging reactive capacity $\mu < \infty$ in case of noncatalytic scavenger.

The definitions must be clarified first. It is established that for selected initial and boundary conditions (steady state solute concentration profile across a passive barrier with fixed boundary concentrations), the lag time for P-film ($\phi = 0$) is not Daynes lag time t_L

$$t_L = \frac{L^2}{6D} \tag{18.1}$$

for the initially solute-free membrane suddenly exposed to the external solute pressure p_{out}, but it is zero because the steady state flux is already established. To distinguish this lag time from Daynes lag time t_L, we call it a *steady state lag time* $t_L^{SS} = t_L^{SS}(\phi)$ due to reaction. The Thiele modulus ϕ can be a constant (for catalytic reactions) or the initial Thiele modulus ϕ_0 for noncatalytic reactions. As stated, for the apparent reaction rate $k = 0, \phi = 0$ and

$$t_L^{SS}(0) = 0 \tag{18.2}$$

For convenience the *reference lag time* $t_{LR} = t_{LR}(\phi)$ is introduced as a separate parameter, even though by the authors' definition for $\phi = 0$ it coincides with Daynes lag time t_L for passive membrane:

$$t_{LR}(0) \equiv t_L \tag{18.3}$$

For a passive membrane the additivity of Daynes and steady state lag times to give the reference lag time t_{LR} may be inferred from Eqs. 18.2 and 18.3:

$$t_{LR}(0) = t_L + t_L^{SS}(0) \tag{18.4}$$

On the other hand, for instantaneous reaction we have from Eqs. 17.12 and 17.13

$$t_L^{SS}(\infty) \equiv t_{LE} = \frac{\mu R_0}{C_{out}} \frac{L^2}{2D} = 3\Psi t_L \tag{18.5}$$

The result of Siegel and Cussler [5] and the authors' numerical simulations to obtain t_{LR} for various large ϕ confirm that for $\phi \to \infty$ the approximate lag time additivity also exists for fast reactions. From this fact and the result in Eq. 18.5 we obtain:

$$t_{LR}(\infty) = t_L + t_L^{SS}(\infty) = t_L(1 + 3\Psi) \tag{18.6}$$

Thus, from analysis of the extreme cases it can be concluded that the reference lag time can be approximately split into purely diffusive and reactive components t_L and $t_L^{SS}(\phi)$, respectively, for any $\phi = [0..\infty]$. Therefore only $t_L^{SS}(\phi)$ has to be analyzed to determine the reference lag time t_{LR} for the initially solute free membrane. In practical applications where the relative scavenging capacity Ψ is large ($\Psi \gg 1$), Daynes lag time contribution can be neglected: then the reference lag time is approximately equal to t_L^{SS}:

$$t_{LR}(\infty) \approx t_L^{SS}(\infty) = 3\Psi t_L \tag{18.7}$$

To analyze the $t_L^{SS}(\phi)$ dependence for non-instantaneous reaction with the apparent rate $0 < k < \infty$, the dynamics of cumulative influx $Q^+(t)$ of the solute into the membrane from the p_{out} side and cumulative efflux $Q^-(t)$ out of the membrane from the p_{in} side must be considered, when the steady state flux across the passive membrane is established by time $t = 0$, and the reaction is homogeneously triggered throughout the membrane at $t = 0$. Figure 3 shows this dynamics for some arbitrary $0 < k < \infty$. Note that the solute efflux $Q^-(t)$ from the membrane may be expressed by the product of previously defined ingress $I(t)$ into the package and the barrier area A:

$$Q^-(t) = I(t)A \tag{18.8}$$

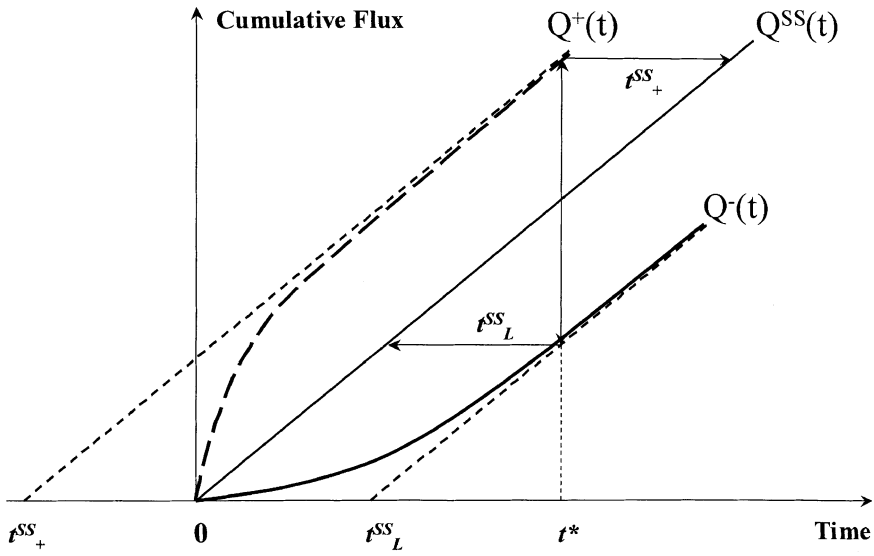

FIGURE 3 Cumulative solute influx and efflux dynamics in R-film with non-instantaneous noncatalytic reaction.

For noncatalytic reaction with finite scavenger reactive capacity μ, this capacity will be completely exhausted at some time t^*. As a result of fixed inner boundary condition $C_{in} = 0$ in the problem formulation, the exact solution for the exhaustion time t^* is infinite. In any practical application the condition $C_{in} = 0$ cannot be maintained exactly because it requires instant removal of permeated solute from the inner boundary and infinitely fine dispersion of scavenger within this boundary. Also, due to localization of the scavenging active sites in polymers, reaction kinetics models based on ideal gas molecular collisions are not fully applicable to solid state reactions, and the kinetic theory for solid permeable catalysts must be invoked. For these two reasons, the actual exhaustion time t^* will be finite. This is expected for noncatalytic reactions, but it makes no difference for the present derivations because all lag time definitions deal with asymptotic behavior at infinite times. Thus t^* may represent any sufficiently long time compared to t_L^{SS}.

Figure 3 shows two characteristic times for any (not necessarily reactive) diffusion driven permeation process at *reference* conditions (initially solute free membrane): the lag time t_L for the solute efflux from inner membrane boundary and the lead time t_+ for the solute influx into film across the outer membrane boundary. Because only *steady state* characteristic times as defined earlier are considered, passive membranes are effectively excluded: for them the corresponding influx and efflux collapse into steady state cumulative flux $Q^{SS}(t)$.

The slopes of asymptotics of both reactive cumulative fluxes $Q^+(t)$ and $Q^-(t)$ are the same and equal to that of $Q^{SS}(t)$ that is constant across any membrane plane x = const, because all three correspond to constant flux $J_{SS} = J_0 = J_L$ across any plane $x =$ const of a passive barrier after scavenger capacity exhaustion at time t^*:

$$J_{SS} = -\frac{DS\Delta p}{L} = -\frac{DC_{out}}{L}, (\text{when } p_{in} = 0) \tag{18.9}$$

The cumulative steady state flux across a passive membrane is found from Eqs. 17.1 and 18.8 as

$$Q^{SS}(t) = -J_{SS}At \tag{18.10}$$

Whereas the equations for $Q^+(t)$ and $Q^-(t)$ asymptotes at $t \to \infty$ are found from Eqs. 17.6 and 18.8 as

$$Q^+(t) = \frac{DC_{out}A}{L}(t - t_+^{SS}) = -J_{SS}A(t - t_+^{SS}) \tag{18.11}$$

$$Q^-(t) = \frac{DC_{out}A}{L}(t - t_L^{SS}) = -J_{SS}A(t - t_L^{SS}) \tag{18.12}$$

where t_+^{SS} is negative. The difference between $Q^+(t^*)$ and $Q^-(t^*)$ is obviously equal to the stoichiometric amount of the solute reacted with the scavenger:

$$Q^+(t^*) - Q^-(t^*) = \mu R_0 AL \tag{18.13}$$

For $\phi \to \infty$ the upper and lower parts of this difference are equal:

$$Q^+(t^*) - Q^{SS}(t^*) = Q^{SS}(t^*) - Q^-(t^*) = \frac{\mu R_0 AL}{2} = \Delta Q \tag{18.14}$$

The result in Eq. 18.14 immediately follows after substituting Eq. 18.5 for t_{LE} into Eq. 18.12 and combining it with Eq. 18.10. Thus, the steady state lead and lag times are equal for instantaneous reaction: $\phi \to \infty$, whereas, obviously, $\Delta Q = 0$ and $t_L^{SS} = 0$ for passive membrane without reaction: $\phi = 0$.

19. LINEAR ANALYSIS OF A SLOW REACTION CASE

To analyze asymptotic behavior of steady state lag and lead times at $\phi \to 0$, it will be assumed that ϕ approaches zero due to infinitely small film thickness L rather than the vanishing apparent reaction rate k. Then the assumption of homogeneous scavenger consumption across the membrane thickness is valid, and the solutions for catalytic reaction can be used for linear analysis provided the scavenger concentration is reduced slowly. Using results from Eqs. 7.1–3 from Part I for catalytic reaction, the solute fluxes across the membrane boundaries $x = 0$ and $x = L$ are

$$J_L = -\sqrt{kD}(\beta_1 - \beta_2) = -\sqrt{kD} \cdot (C_{out}\coth(\phi_0) - C_{in}\operatorname{csch}(\phi_0)) \tag{19.1}$$

$$J_0 = -\sqrt{kD} \cdot (c_{out}\operatorname{csch}(\phi_0) - C_{in}\coth(\phi_0)) \tag{19.2}$$

where ϕ_0 is the initial Thiele modulus for the reactive layer in case of noncatalytic reaction rather than constant ϕ for a catalytic one. Taking into account the earlier assumption $C_{in} = 0$, the steady state flux across passive membrane J_{SS} from Eq. 18.9, and expanding the exponents in Eqs. 19.1,2 into Taylor series around $\phi_0 = 0$ truncated at $o(\varphi_0^3)$, the reactive fluxes are expressed as

$$J_L = -\frac{DC_{out}}{L} \cdot \frac{\phi_0(e^{\phi_0} + e^{-\phi_0})}{e^{\phi_0} - e^{-\phi_0}} \cong J_{SS}\frac{\phi_0(2 + \phi_0^2)}{2\phi_0 + \frac{\phi_0^3}{3}} \cong J_{SS}\left(1 + \frac{\phi_0}{2} - \frac{\phi_0^2}{6}\right) \tag{19.3}$$

$$J_0 = -\frac{DC_{out}}{L} \cdot \frac{2\phi_0}{e^{\phi_0} - e^{-\phi_0}} \cong J_{SS} \frac{2\phi_0}{2\phi_0 + \frac{\phi_0^3}{3}} \cong J_{SS}\left(1 - \frac{\phi_0^2}{6}\right) \tag{19.4}$$

Because the reactive layer thickness $L \to 0$ and scavenger consumption is homogeneous across the thickness, the scavenger capacity will be exhausted at some time $t = t^*$ throughout the membrane. Then the transition from reactive to passive permeation will occur simultaneously at both membrane boundaries. Substituting Eqs. 19.3 and 19.4 into Eq. 17.1, converting them into cumulative fluxes following Eq.18. 8 and equaling them to Eqs. 18.11 and 18.12, respectively, the system of two linear equations is obtained, matching passive and linearized reactive cumulative flux dynamics at time t^* as shown in Figure 4 for some small ϕ_0 value:

$$Q^+(t^*) = -J_{SS}A\left(1 + \frac{\phi_0}{2} - \frac{\phi_0^2}{6}\right)t^* = -J_{SS}A(t^* - t_+^{SS}) \tag{19.5}$$

$$Q^-(t^*) = -J_{SS}A\left(1 - \frac{\phi_0^2}{6}\right)t^* = -J_{SS}A(t^* - t_L^{SS}) \tag{19.6}$$

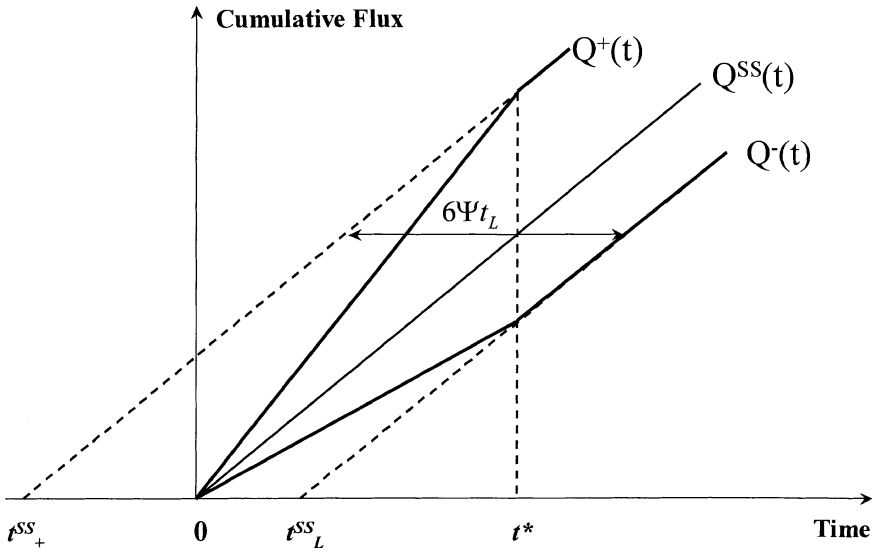

FIGURE 4 Linear analysis of cumulative flux dynamics for $\phi_0 \to 0$.

Subtracting Eq. 19.6 from Eq. 19.5 and using Eq. 18.13, t^* is found as

$$t^* = \frac{L^2}{D}\frac{2\mu R_0}{C_{out}\phi_0} = \frac{L^2}{D}\frac{2\Psi}{\phi_0} \tag{19.7}$$

Now the lead and lag time asymptotics at $\phi_0 \longrightarrow 0$ are obtained from matching relationships (Eq. 19.5 and 19.6) for cumulative flux by substituting the result in Eq. 19.7 into them:

$$t_+(\phi_0 \longrightarrow 0) = \left(\frac{\phi_0^2}{6} - \frac{\phi_0}{2}\right)t^* = \frac{L^2}{D}\frac{\mu R_0}{C_{out}}\left(\frac{\phi_0}{3} - 1\right) = 2\Psi(\phi_0 - 3)t_L \tag{19.8}$$

$$t_L(\phi_0 \longrightarrow 0) = \frac{1}{6}\phi_0^2 t^* = \frac{L^2}{3D}\frac{\mu R_0}{C_{out}}\phi_0 = 2\Psi\phi_0 t_L \tag{19.9}$$

where t_L is Daynes lag time (Eq. 18.1), that is the reference lag time for a passive membrane. The result in Eq. 19.9 proves that the steady state lag time does go to zero at $\phi_0 \longrightarrow 0$ with the slope $2\Psi t_L$ at least for very thin films. This trend seems to be confirmed by the authors' limited numerical simulations; however, these simulations cannot be used as a concept proof because at small ϕ_0 the time to completely exhaust the scavenger reactive capacity goes to infinity. Therefore, obtaining true steady state lead and lag times would require excessive simulation times. This situation is not of practical importance either, because small ϕ_0 translates into negligible barrier performance gains. The presented linear analysis may not be adequate if $\phi_0 \longrightarrow 0$ trend is due to small apparent reaction rate k only, and the assumption of homogeneous reaction across membrane thickness is invalid. It does show, however, that the smooth transition between purely passive and reactive steady state lag times $t_L^{SS}(0) = 0$ and $t_L^{SS}(\infty) = 3\Psi t_L$, respectively, hypothesized by Cussler and Yang in Reference 3, is possible at least for some specific conditions. That transition occurs between steady state lag times 0 and $3\Psi t_L$ rather than t_L and $3\Psi t_L$ as sought by Cussler and Yang because they tried to compare reference lag time for passive membrane with steady state lag time for a reactive one without distinguishing between the two. With steady state lag time definitions in place, $t_L^{SS}(\phi)$ does go to zero when the initial scavenger concentration R_0 is reduced, and there is no need for Cussler's hypothesis of uniform linear dependence of t_L^{SS} on ϕ for $\phi = [0..\infty]$.

A useful relationship between the lead and lag times for noncatalytic reactions with any $k > 0$ is obtained by substituting Eqs. 18.11 and

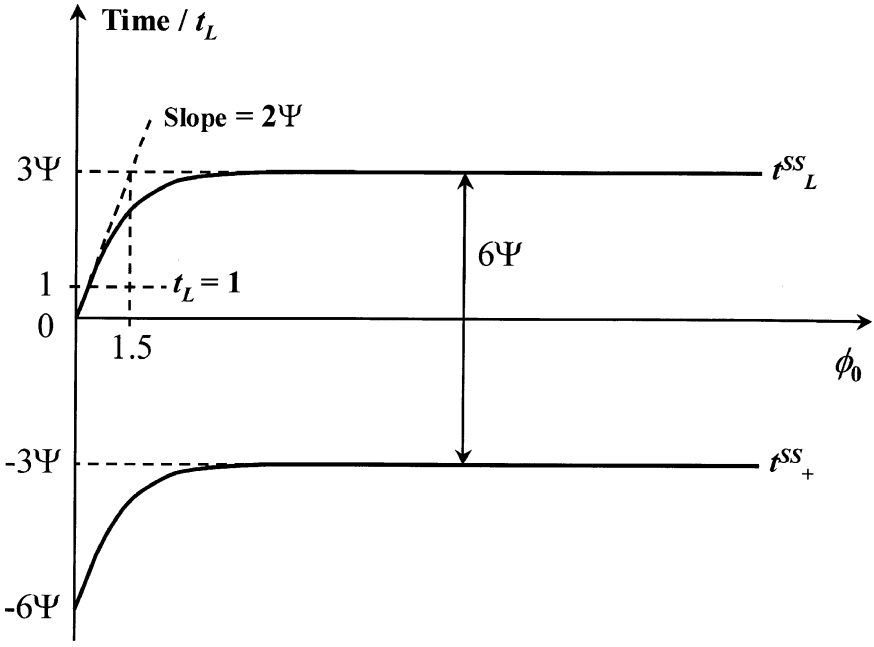

FIGURE 5 Lead and lag times as a function of the intial Thiele modulus.

18.12 into Eq. 18.13, or equivalently from Eqs. 19.8 and 19.9:

$$t_L^{SS} - t_+^{SS} = \frac{\mu R_0 L^2}{DC_{out}} = 6\Psi t_L \tag{19.10}$$

Figure 5 demonstrates the lead and lag trends within the described applicability limits. Note that the constant lag and lead time separation of $6\Psi t_L$ is present for any $\phi_0 > 0$. From the slope of $t_L^{SS}(\phi_0)$ trend at $\phi_0 \longrightarrow 0$ found according to Eq. 19.9 it is concluded of that $\phi_0 = 1.5$ will be a point below which a significant deviation of the steady state lag time from the result in Eq. 14.1 for t_{LE} at $\phi_0 \to \infty$ will occur. This result also confirms that for systems where the reaction is the rate-determining step with $\phi_0 \ll 1$ or the joint activation-diffusion control is exercised as in case of $\phi(t) < \phi_0 = 1.5$, the concept of lag time as a characteristic system property becomes mostly irrelevant. The underlying reason for that conclusion is that there is no value in studying asymptotic behavior of the system that only approaches steady state at infinite times. Such a system has an infinitely long transient phase with no true asymptotic behavior.

20. SG MODEL LAG TIME

Considering the points made in the preceding section regarding the steady state lag time t_L^{SS} dependence on the initial Thiele modulus ϕ_0, it is seen that the approximate character of the SG model for intermediate values of ϕ_0 will not provide a reliable way to estimate cumulative solute efflux asymptotics at infinite times, necessary for determining the steady state lag time. The main reason is that the SG model truncates the infinite scavenger exhaustion time to finite t_E^+ for any initial Thiele modulus ϕ_0. Therefore, any SG model lag time predictions will be a valid approximation only around total permeation time equal to t_E^+. Because $t_E^+ \leq 2t_{LE}$ for any $\phi_0 > 0$, the scavenger exhaustion lag time t_{LE} may serve as an engineering estimate of time during which SG model predictions of the solute ingress and the steady state lag time can be used.

The SG model steady state lag time t_L^+ for the R-film with noncatalytic scavenger has to asymptotically satisfy the downstream concentration growth equation after the exhaustion of scavenger reactive capacity, that is, for $t > t_E^+$:

$$[C]_{in}(t)\frac{V}{A} = I(t) = -J_{SS}(t - t_L^+) \tag{20.1}$$

Here V is the volume of the downstream chamber, $[C]_{in}$ is the permeant concentration in the chamber, and A is the area of the barrier. Substituting the solution in Eq. 17.10 for the ingress $I_R^+(t_E^+)$ into Eq. 20.1 we obtain for t_L^+:

$$t_L^+ = t_E^+ + \frac{I(t_E^+)}{J_{SS}} \tag{20.2}$$

that in the case of $P_{in} = 0$ results in

$$t_L^+ = \frac{\mu R_0}{kSp_{out}}\left[\frac{\phi_0^2}{2} - \phi_0 + \ln\left(\frac{1+e^{2\phi_0}}{2}\right) - \frac{2\phi_0^2}{(1+\phi_0)} \times\left(\arctan\left(e^{\phi_0}\right) - \frac{\pi}{4} - \frac{e^{\phi_0}}{\phi_0\left(1+e^{2\phi_0}\right)} + \frac{1}{2\phi_0}\right)\right] \tag{20.3}$$

Figure 6 demonstrates that the solution in Eq. 20.3 for noncatalytic reactive membrane, although not representative of the system asymptotics at infinite time, provides a good approximation of the "transient" steady state lag time t_L^{SS} around the SG model exhaustion time t_E^+ for $\phi_0 > 2$. For these values of the initial Thiele modulus ϕ_0, the SG model exhaustion time t_E^+ represents the time when the scavenging reaction

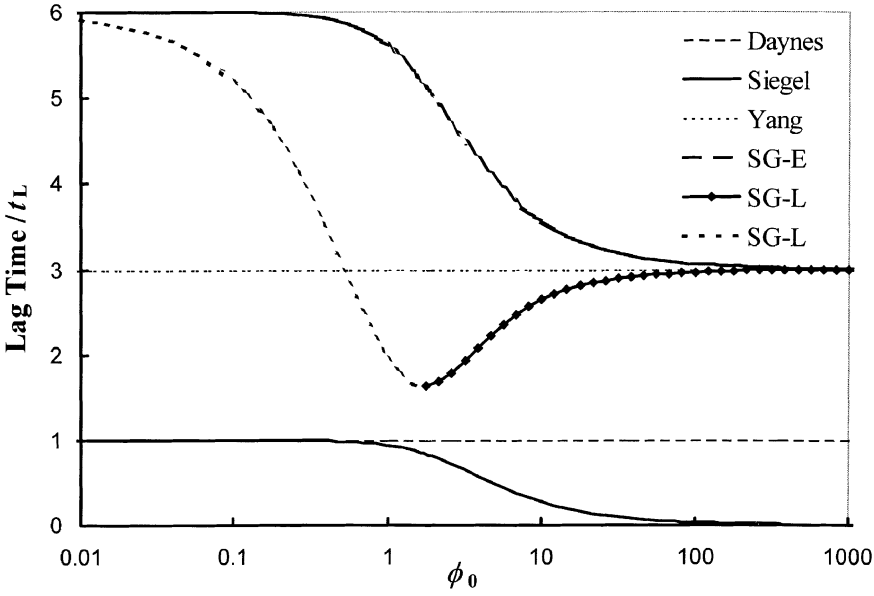

FIGURE 6 Lag time prediction comparison of various models (SG model lag time represents a measure of reactive barrier performance around t_E^+).

is mostly completed. As such, the result in Eq. 20.3 along with Eq. 17.10 forms a useful engineering tool for analyzing transient barrier performance during the active scavenging period most critical for reactive barrier design.

21. EXPERIMENTAL ESTIMATION OF THE SCAVENGING RATE

Earlier it was assumed that the solute scavenging reaction is diffusion controlled, that is, that the apparent reaction rate is limited not by reaction activation kinetics upon solute molecule collision with the reactive site but rather by diffusive transport of the solute to reactive sites. Although other methods of measuring the reaction rate were proposed [3,6], this section focuses on the most direct method applicable to particulate scavenger subsequently dispersed in a polymer matrix. Placing the activated scavenger particulate into a sealed gas chamber with oxygen sensor and filling it with oxygen in the absence of convection allows the measurement of the kinetics of oxygen consumption and determines the initial reaction rate k_0 when the excess

scavenger concentration $R = R_0$ can be assumed:

$$\frac{\partial C}{\partial t}\Big|_{t=0} = -\mu K_d R_0 C_0 = -K_0 C_0 \tag{21.1}$$

The meaning of the scavenger concentration R_0 for a particulate not dispersed in a continuous medium is simply the amount of the activated scavenger N_S per test chamber volume V:

$$R_0 = \frac{N_s}{V} \tag{21.2}$$

From the principles of molecular reaction dynamics [7] the diffusion controlled reaction rate constant K_d can be expressed as a function of diffusivity D:

$$K_d = 4\pi R_g N_A D_s \tag{21.3}$$

$$k_0 = \mu K_d R_0 \tag{21.4}$$

where R_g is the universal gas constant, N_A is Avogadro constant, and D_s is the self-diffusion coefficient of the gaseous permeant in vacuum. Then the reaction rates K and k in a solid polymer can be found from Eqs. 21.2 and 21.3 as

$$K = K_d \frac{D_p}{D_s} = k_0 \frac{D_p}{D_s \mu R_0} \tag{21.5}$$

$$k = \mu K R_p = k_0 \frac{D_p R_p}{D_s R_0} \tag{21.6}$$

where R_0 is found from Eq. 21.2, D_p is the permeant diffusivity in solid polymer, R_p is the initial scavenger concentration in the reactive film. k_0 is found from the experimental data using Eq. 21.1 as

$$k_0 = \frac{dC}{dt}\Big|_{t=0} \Big/ C_0 \tag{21.7}$$

Formulas 21.6 and 21.7 provide a tool for determining the apparent reaction rate constant k from controlled experimental data for scavenger particulate in oxygen atmosphere. It should be noted that morphology and activation mechanism of scavenger must be exactly the same in the gas chamber experiment and in the reactive film because R actually stands for concentration of active scavenging sites assuming unhindered access of oxygen to them. Therefore, for the same amount of scavenger the same active surface area (i.e., morphology) must be provided if it is to be assumed that the reaction is occurring mostly on the surface of the particulate.

To estimate the scavenging reactive capacity μ, the experiment should be allowed to run for a sufficiently long time to completely deactivate the scavenger. Then μ is obtained as a total amount of consumed oxygen (e.g., as scavenging substrate weight gain) divided by the initial amount of the scavenger N_s in the chamber.

22. EFFECT OF FILM THICKNESS ON BARRIER PERFORMANCE OF R- AND P-FILMS

For P-film the effect of thickness on J_0 and TR_{eff} is given by Eq. 6.3 and 6.5 in Part I, respectively. For R-film these quantities are given by Eq. 7.4 and 7.5 for the catalytic scavenger. Figure 7 demonstrates the effective steady state flux dependence on the film thickness L for the special case $C_{in} = 0$ and fixed values of k, D, and S. The effective flux dynamics for consumable scavenger was shown in Figures 8 and 9 in Part II, hence the steady state results reported here for the catalytic scavenger refer to the initial effective flux $J_0(0)$ for the consumable one. The flux $J_0(0)$ is a good approximation of R-film performance during the exhaustion lag time t_{LE} when the initial Thiele modulus of the reactive layer is sufficiently large: $\phi_0 \gg 1$.

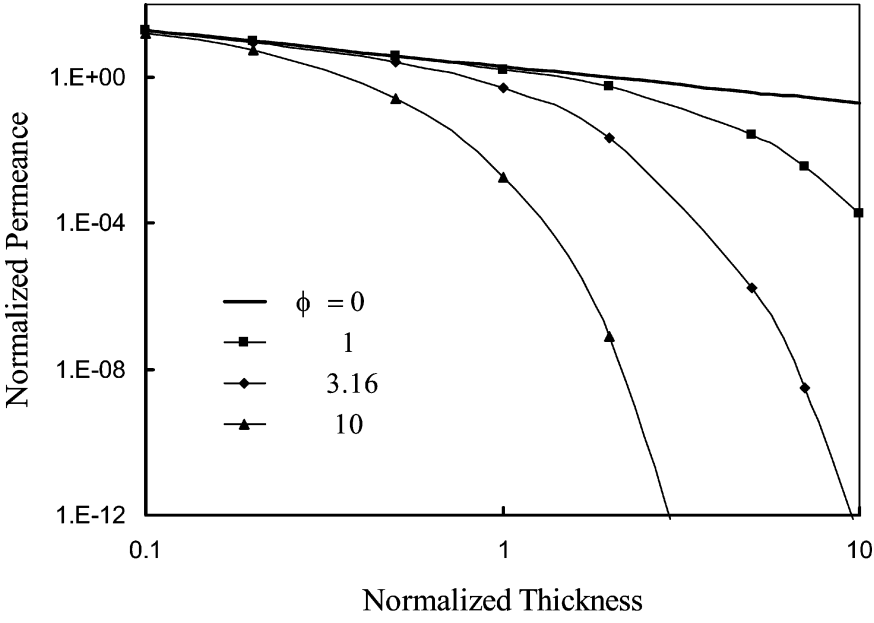

FIGURE 7 Dependence of R-film initial permeance on film thickness.

Doubling P-film thickness reduces the effective flux through it by a factor of 2. Doubling R-film thickness reduces the initial effective flux J_0 by a factor of $\sinh(2\phi_0)/\sinh(\phi_0)$, which for $\phi_0 < 1$ (slow reaction) is reduced to 2 $\cosh(\phi_0)$. It is noted that this result contradicts the common belief that reactive films with *fast reaction* exhibit effective transmission rate dependence on thickness similar to passive films, while it is true for slow reactions.

23. EFFECTS OF DIFFUSIVITY AND SOLUBILITY FOR R-AND P-FILMS

Table 1 summarizes the findings for relative performance of P- and R-films with intermediate initial Thiele moduli ϕ_0 varying from 1 to 31 and relative scavenging capacity Ψ varying from 5 to 500 to demonstrate the difference between Yang-Nuxoll-Cussler (YNC) and Solovyov-Goldman (SG) exhaustion times t_{LE} and t_E^+, respectively, and compares the transient solute ingress through the films with different material properties. Larger initial Thiele moduli would result in a more dramatic transient transmission rate reduction: exploring these cases is left as an exercise for the reader. Also, the difference between t_{LE} and t_E^+ becomes negligible for $\phi_0 > 100$.

In Table 1 the effective flux J_0 for R-film is shown at $t = 0$ as it increases with time until it reaches the steady state flux J_P for P-film at $t = \infty$. Factor $\gamma = J_P/J_0$ demonstrates the relative initial barrier improvement for R-film compared to P-film. Parameter $\gamma = \gamma(t)$ will decrease with time as J_0 increases, but the rate of J_0 increase with time is slow for fast reactions during most of the exhaustion lag time as shown in Figure 8 of Part II. Note that reported γ values refer only to the SG model: γ cannot be determined from the YNC model because it postulates an impermeable reaction wavefront during the exhaustion lag time resulting in $J_0(0..t_{LE}) = 0$. In Table 1 all exhaustion and lag time estimates are in days: commonly used dimensionless time Dt/L^2 is not utilized because it is not a representative quantity for R-films where the exhaustion time is largely controlled by the scavenger reactive capacity μR_0 and the external permeant pressure p_{out} through parameter Ψ rather than by diffusivity D and thickness L of the film material that control the reference lag time. The solute ingress values are in [$\mathrm{cm^3(STP)m^{-2}}$] during specified time t_E^+. Total scavenger load R_0AL in the film is the same for all cases (except case 8 where it is doubled). Thus, the scavenging capacity of the film unit volume is set as $\mu R_0 = 1$ [$\mathrm{m^3(STP)\ m^{-3}}$] for all cases except case 7 where $\mu R_0 = 0.5$ to preserve the constant total scavenger loading. $\mu R_0 = 1$ is also used for case 8 with double thickness.

TABLE 1 Solute Ingress and Initial Flux through P- and R-films and Corresponding Exhaustion and Lag Times for R-film

Case no.	1	2	3	4	5	6	7*	8	9	10
D	1	0.1	10	0.1	1	0.1	1	1	1	1
S	1	10	0.1	1	0.1	0.1	1	1	1	1
L	1	1	1	1	1	1	2	2	1	1
k	10	10	10	10	10	10	10	10	100	1000
ϕ_0	3.162	10	1	10	3.162	10	6.325	6.325	10	31.623
Ψ	50	5	500	50	500	500	25	50	50	50
Performance Properties										
J_0	5.36E-01	1.82E-03	1.702	1.82E-04	5.36E-02	1.82E-05	2.27E-02	2.27E-02	1.82E-03	2.34E-12
J_P	2.000	2.000	2.000	0.200	0.200	0.020	1.000	1.000	2.000	2.000
γ	3.729	1101.3	1.175	1101.3	3.729	1101.3	44.122	44.122	1101.3	8.56E + 11
t_{LE}	2.894	2.894	2.894	28.935	28.935	289.352	5.787	11.574	2.894	2.894
t_E^+	4.323	3.432	5.404	34.321	43.234	343.211	7.416	14.833	3.432	3.073
$I(t_E^+)$	42.66	15.19	60.89[1]	15.19	42.66	15.19	23.55	47.10	15.19	4.91
t_L^+	1.855	2.553	1.880	25.532	18.546	255.317	4.691	9.382	2.553	2.788

Reactive Capacity of the Film $\mu R_0 = 1[\mathrm{m}^3(\mathrm{STP})\mathrm{m}^{-3}]$ except in case 7* where $\mu \mathrm{R}_0 = 0.5$. [1]$\phi_0 = 1$ in case 3: the SG model underpredicts the actual ingress for $\phi_0 < 2$ (approximately by 30% in this case).

Comparing cases 1,2, and 3 it is observed that permeability $P = DS$ of P-films (as a property of passive material and the nature of the solute) as well as corresponding flux J_P are the same whereas D and S values are varied. There is a large difference in the initial effective flux J_0 through R-film as demonstrated by the barrier improvement ratio γ. Material 2 with the lowest diffusivity D provides the best transient barrier improvement, whereas material 3 with the highest diffusivity provides almost no improvement in terms of SG model lag time t_L^+ and significantly higher solute ingress during comparable exhaustion time t_E^+. The SG model lag time t_L^+ is also improved for material 2 compared to 1 and 3.

The effects of separate improvements in material parameters D and S are shown in cases 4–6 and again it is seen that lowering the diffusivity value D is the preferred way of improving transient barrier performance.

Comparing cases 2 and 9 it is noted that increasing scavenger reactivity k tenfold is equivalent to simultaneously reducing D and increasing S tenfold, whereas comparing case 9 with case 1 a large increase in transient barrier performance is seen in case of a higher reaction rate accompanied by some extension of the SG model lag time.

Increasing the film thickness twofold as shown in cases 7 and 8 with the same total amount of scavenger per film and the same scavenger concentration in film, respectively, reduces the initial solute flux by a factor $\sinh(2\phi_0)/\sinh(\phi_0)$ and also more than doubles the SG model lag time in case 7 for the same amount of scavenger used compared to case 1.

Reducing the permeant solubility S in the film material tenfold (compare cases 1 and 5) does not affect initial barrier improvement factor γ but increases the scavenger lifetime to obtain the same solute ingress in proportional to solubility reduction factor.

24. SUMMARY

Parts I–III of this series developed the analytical theory of transient permeation through reactive barrier films containing noncatalytic immobile scavenger able to irreversibly bind permeating solute upon its activation. The theory is validated for the initial Thiele modulus of the reactive layer $\phi_0 > 2$, and it predicts the effective transmission rates of the solute through the film as a function of time, transient solute ingress into a package, and the useful life of the scavenger depending on matrix polymer properties, the boundary conditions, reactivity, and reactive capacity of the scavenger. It is shown that synergistic effects of permeant diffusivity, solubility in film material, and scavenger reactivity on the transient barrier performance are controlled by two independent dimensionless parameters: the initial Thiele

modulus ϕ_0 for the homogeneous reactive monolayer and the relative scavenging capacity Ψ of the film that also depends on the external solute pressure. It was also demonstrated that placing scavenger within the passive barrier material with the lowest diffusivity greatly enhances barrier performance by lowering transient solute ingress. Placing the scavenger within the passive barrier with the same material permeability achieved by lower permeant solubility in it results in negligible performance gains for practical packaging applications.

NOTATION

A	area of the barrier (exposed package surface area)
a	$\equiv C_{in}$
B	integration constant
b	$\equiv C_{out}$
C	concentration of permeant in film material
$[C]$	concentration of permeant in gas phase (outside the film)
C_{in}	equilibrium permeant concentration within the downstream film boundary $x = 0$
C_{out}	equilibrium permeant concentration within the upstream film boundary $x = L$
$C^*(x)$	instantaneous permeant concentration profile assuming established R profile
c_1	$\equiv \exp(\phi_1)$
c_2	$\equiv \exp(\phi_2)$
D	permeant diffusivity in film layer (also D_p)
D_s	self-diffusion coefficient of permeant in vacuum
Da^{II}	Second Damkohler number for reactive layer
d	$\equiv S_1/S_2$
e_1	$\equiv \sqrt{k_1 D_1}$
e_2	$\equiv \sqrt{k_2 D_2}$
f_1	$\equiv L_1/D_1$
f_2	$\equiv L_2/D_2$
$I(t)$	permeant ingress into the package across a unit film area during time t
J_0	effective permeant flux across downstream boundary $x = 0$ of barrier film
J_f	permeant flux into moving reaction wavefront
J_P	permeant flux through homogeneous passive barrier
J_{PP}	permeant flux through passive-passive barrier (two layer film)
J_{SS}	steady state permeant flux through homogeneous passive barrier, same as J_P
J_x	permeant flux across film plane $x = \text{const}$

H	partition coefficient of permeant in film material relative to external medium
$h(t)$	Heaviside step function
K	reaction rate constant for permeant consumption by scavenger
K_A	reaction rate constant for fully activated scavenger at 100% capacity
k	pseudo first order apparent reaction rate constant for the reactive layer ($= \mu K R_0$)
L	membrane layer thickness
L_d	position of reaction wavefront propagating downstream
L_d^*	position of reaction wavefront propagating downstream relative to outer film boundary $x = L$
L_u	position of reaction wavefront propagating upstream
N_A	Avogadro constant
N_S	amount of scavenger (as moles of active sites)
P	permeability coefficient of particular permeant in film material
p	partial pressure of gaseous permeant
p_{in}	partial pressure of gaseous permeant inside the package
p_{out}	partial pressure of gaseous permeant outside the package
$Q^+(t)$	cumulative solute influx into the film across outer boundary $x = L$
$Q^-(t)$	cumulative solute efflux from the film across inner boundary $x = 0$
$Q^{SS}(t)$	cumulative solute flux across any plane $x = \text{const}$ of passive membrane at steady state permeation conditions
R	concentration of scavenger in film material
R_0	initial concentration of scavenger in film material
R_g	the universal gas constant
r_{HS}	rate of scavenging of permeant present in package headspace
S	solubility coefficient of particular permeant in film material
T	temperature
t	time
t_+	reference lead time for passive barrier
t_+^{SS}	steady state lead time for noncatalytic reactive barrier
t_E^+	SG model scavenger exhaustion time for the initial Thiele modulus $\phi_0 > 2$
t_L	reference lag time for passive barrier
t_{LR}	unified reference lag time for passive and reactive barriers
t_L^{SS}	steady state lag time for noncatalytic reactive barrier
t_L^+	SG model steady state lag time for reactive barrier

t_{LE} YNC scavenger exhaustion lag time when the initial Thiele modulus $\phi_0 \to \infty$
TR transmission rate of permeant through a particular film
TR_{eff} effective transmission rate measured at the downstream boundary of the film
$\overline{TR}_{eff}$ alternatively defined effective transmission rate when $0 < p_{in} \cong p_{out}$
x coordinate across film thickness L
x^* coordinate across film thickness reciprocal to x: $x^* = L - x$
Y $\equiv \exp\left(2L_d(t)\sqrt{\frac{k}{D}}\right) = \exp(2(\phi_0 - Z))$
Z reciprocal Thiele modulus $(=\phi_0 - \phi_R)$ for partially reacted reactive-passive structure

GREEK SYMBOLS

β_1, β_2 coefficients in steady state solution of reaction-diffusion problem for permeant concentration in reactive layer (determined from boundary conditions)
γ active barrier improvement ratio (ratio of passive flux to effective reactive flux)
δ determinant of a matrix
μ Refreactive capacity of scavenger (moles of solute per mole of scavenger)
ϕ Thiele modulus for reactive layer (same as Hatta number Ha)
ϕ_0 initial Thiele modulus for reactive layer with $R(x,t) \neq$ const
ϕ_R transient Thiele modulus for reactive layer with moving reaction zone
ξ dimensionless x coordinate across film thickness
Ψ relative scavenging capacity of film material

REFERENCES

[1] Solovyov, S. E. and Goldman, A. Y. Theory of Transient Permeation Through Reactive Barrier Films I. Steady State Theory for Homogeneous Passive and Reactive Media, *Int. J. Polym. Mat.* (this issue).
[2] Solovyov, S. E. and Goldman, A. Y. Theory of Transient Permeation Through Reactive Barrier Films II. Two Layer Reactive-Passive Structures with Dynamic Interface, *Int. J. Polym. Mat.* (this issue).
[3] Cussler, E. L. and Yang, C. (2000). *TAPPIJ*. **83**, 106.
[4] Yang, C., Nuxoll, E. E. and Cussler, E. L. (2001). *AIChE J.* **47**, 295.
[5] Siegel, R. A. and Cussler, E. L. (2004). *J. Membr. Sci.* **229**, 33.
[6] Seeper, D. V., Morgan, C. R., Roberts, W. P. and van Putte, A. W., U.S. Patent 5,529, 833 (1996).
[7] Atkins, P. W. and de Paula, J. (2001). *Physical Chemistry, 7th ed.*, (W. H. Freeman Co., New York).